

Chemical trends for defect energy levels in  $\text{Hg}_{(1-x)}\text{Cd}_x\text{Te}$ 

Akiko Kobayashi, Otto F. Sankey, and John D. Dow

*Department of Physics and Materials Research Laboratory, University of Illinois at Urbana-Champaign, 1110 West Green Street, Urbana, Illinois 61801*

(Received 23 November 1981)

The chemical trends for the energy levels of  $sp^3$ -bonded substitutional defects in  $\text{Hg}_{(1-x)}\text{Cd}_x\text{Te}$  are predicted and appear to be in general agreement with what is known about defect levels in this small-band-gap semiconductor alloy.

## I. INTRODUCTION

The purpose of this paper is to present a theory of the chemical trends for substitutional  $sp^3$ -bonded deep-trap energy levels in  $\text{Hg}_{(1-x)}\text{Cd}_x\text{Te}$ .  $\text{Hg}_{(1-x)}\text{Cd}_x\text{Te}$  is a variable-band-gap zinc-blende semiconductor that has important potential applications in infrared photodetection. Its band gap varies continuously as a function of alloy composition  $x$  from 1.59 eV in CdTe ( $x = 1.0$ ) to zero for  $x \simeq 0.16$ ; HgTe is a semimetal. The most carefully studied alloy compositions range from  $x = 0.2$  to 0.4. Traps associated with defects or impurities degrade the performance of  $\text{Hg}_{(1-x)}\text{Cd}_x\text{Te}$  electronic devices (i) by providing unwanted recombination paths and (ii) by permitting undesirable noise currents associated with valence electrons being thermally excited first to the trap level and then to the conduction band.<sup>1</sup> Efforts to improve the quality of device-grade  $\text{Hg}_{(1-x)}\text{Cd}_x\text{Te}$  are hampered by the problem of first identifying the defects responsible for the unwanted trap levels and then either removing the defects or altering the material so that the trapping properties are suitably modified.

The small band gap 0.1–0.3 eV of the technologically important  $\text{Hg}_{(1-x)}\text{Cd}_x\text{Te}$  presents a serious obstacle to the interpretation of defect levels in the gap, however. Most theories of “deep” traps are uncertain by several tenths of an eV, and at first examination would appear to be incapable of assisting in the interpretation of data. Indeed, the conventional definition of a “deep” level is that it lies more than 0.1 eV from the nearest band edge; a definition that is meaningless in a 0.2-eV band-gap material. Progress can be made, however, if we adopt the more recent theoretical and experimental definitions of a “deep” level<sup>2</sup> as one that (i) is bound by the defect’s central-cell potential and (ii) does not necessarily follow the band edges as

the host alloy composition is varied. The data of Jones *et al.*<sup>1</sup> reveal two such deep levels in  $\text{Hg}_{(1-x)}\text{Cd}_x\text{Te}$ . While a 0.2-eV uncertainty theory cannot predict with confidence which defects are responsible for the observed deep levels, it can exclude many possible defects as candidates and it can exhibit the chemical trends in the deep-trap energies to be expected as the host alloy composition is varied and as the impurities are changed. Such an imprecise theory, if sufficiently global in its predictions, can be useful for formulating and testing hypotheses concerning defect levels. In this paper we present such a theory.

## II. THEORY

The theory draws heavily on ideas advanced for  $\text{GaAs}_{1-x}\text{P}_x$  by Hsu *et al.*<sup>3</sup> and on the theory of deep levels in III-V semiconductors by Hjalmarson *et al.*<sup>2</sup> We seek to solve the Schrödinger equation for the substitutional defect energy levels  $E$ :

$$\det[1 - (E - H_0)^{-1}V] = 0 \quad (1a)$$

or

$$\det[1 - G_0(E)V] = 0 \quad (1b)$$

Here  $V$  is the defect-potential operator,  $H_0$  is the host Hamiltonian operator, and  $G_0(E) = (E - H_0)^{-1}$  is the perfect-crystal Green’s function. Solution of the Schrödinger equation is greatly simplified by an apt choice of basis, as constructed by Vogl *et al.*<sup>4</sup> for III-V semiconductors. Two significant differences exist between the III-V’s and  $\text{Hg}_{(1-x)}\text{Cd}_x\text{Te}$ , however. Both HgTe and CdTe have strong spin-orbit coupling, which must be included, and the band gap of  $\text{Hg}_{(1-x)}\text{Cd}_x\text{Te}$  vanishes for  $x \simeq 0.16$ ; hence the host-crystal Hamiltonian  $H_0$  must be treated carefully.

Following the general ideas of Harrison,<sup>5</sup> Chadi,<sup>6</sup> and Vogl *et al.*,<sup>4</sup> we construct the empirical tight-binding Hamiltonian:

$$H_0 = \sum_{\vec{R}, \sigma, i} ( |a, i, \sigma, \vec{R}\rangle E_{i,a} \langle a, i, \sigma, \vec{R}| + |c, i, \sigma, \vec{R} + \vec{d}\rangle E_{i,c} \langle c, i, \sigma, \vec{R} + \vec{d}| ) \\ + \sum_{\vec{R}, \vec{R}', \sigma, i, j} [ |a, i, \sigma, \vec{R}\rangle V_{i,j}(\vec{R}, \vec{R}' + \vec{d}) \langle c, j, \sigma, \vec{R}' + \vec{d}| + \text{H.c.} ] + H_{s_0} . \quad (2)$$

Here H.c. means Hermitian conjugate,  $\vec{R}$  are the face-centered-cubic lattice positions of the anions,  $i$  and  $j$  are the basis orbitals  $s, p_x, p_y, p_z$ , and  $s^*$ ,  $\sigma$  is the spin ( $\uparrow$  or  $\downarrow$ ),  $a$  and  $c$  represent the anion and cation, respectively, and  $\vec{d}$  is the position of the cation relative to the anion in the  $\vec{R}$ th cell:  $\vec{d} = (a_L/4)(1,1,1)$ . The anion (cation) orbital with quantum number  $i$  and spin  $\sigma$  centered at  $\vec{R}$  ( $\vec{R} + \vec{d}$ ) is  $|a, i, \sigma, \vec{R}\rangle$  ( $|c, i, \sigma, \vec{R} + \vec{d}\rangle$ ). In this model, the off-diagonal matrix elements  $V$  vanish unless  $\vec{R}$  and  $\vec{R}' + \vec{d}$  refer to nearest-neighbor atoms. The spin-orbit Hamiltonian is

$$H_{s_0} = \sum_{\vec{R}, \sigma, \sigma', i, j} ( |a, i, \sigma, \vec{R}\rangle 2\lambda_a \vec{L}_a \cdot \vec{\sigma}_a \langle a, j, \sigma', \vec{R}| + |c, i, \sigma, \vec{R} + \vec{d}\rangle 2\lambda_c \vec{L}_c \cdot \vec{\sigma}_c \langle c, j, \sigma', \vec{R} + \vec{d}| ) . \quad (3)$$

$H_{s_0}$  in this atomiclike local basis is an off-diagonal matrix which couples the different spin states with the  $p$  states on the same atom.

We have used an  $sp^3s^*$  basis of five orbitals per atom; the  $sp^3$  part of the basis is necessary to obtain correct covalent bonding, and the excited  $s$  state  $s^*$  is useful for simulating the higher energy excited states in the conduction bands. The parameters of the model for HgTe and CdTe are listed in Table I. These parameters were determined by fitting the pseudopotential band structures of HgTe (Ref. 7) and CdTe (Ref. 8) at the  $\Gamma$  ( $\vec{k} = \vec{0}$ ) and  $X$  [ $\vec{k} = (2\pi/a_L)(1,0,0)$ ] points, where the Hamiltonians are block-diagonal. In the case of HgTe, the lowest valence bands were fitted to photoemission data,<sup>9</sup> because these bands were not included in Ref. 7. The spin-orbit parameters  $\lambda_a$  and  $\lambda_c$  were determined from the  $\Gamma$  point splittings of the band structures at  $\Gamma_7$  and  $\Gamma_8$ . (Appendix A contains details of the band-structure fitting procedure.)

The band structures of the alloys were obtained using the virtual-crystal approximation, with the Hamiltonian matrix elements being linearly interpolated as functions of  $x$ .<sup>10</sup> Values of the energy at high-symmetry points in the band structure are tabulated in Table II. The resulting alloy band structures for  $x = 0, 0.16$ , and  $1$  are plotted in Figs. 1, 2, and 3, respectively. The host spectral density operator  $\delta(E - H_0)$  and the Green's function  $G_0(E) = (E - H_0)^{-1}$  can then be evaluated from the band structure, using established procedures.<sup>2</sup> The defect potential can be formed as by Hjalmarson *et al.* for III-V's. The on-site matrix elements of the host Hamiltonian are approximated by

$$E_{s,a} - E_{s,c} = \beta_s (E_{s,a}^{(\text{atom})} - E_{s,c}^{(\text{atom})}) \quad (4a)$$

and

$$E_{p,a} - E_{p,c} = \beta_p (E_{p,a}^{(\text{atom})} - E_{p,c}^{(\text{atom})}) , \quad (4b)$$

where the superscript (atom) refers to the free atomic orbital energy. A good fit to the band structures of HgTe and CdTe is obtained with the proportionality constants  $\beta_s$  and  $\beta_p$ , chosen to be

TABLE I. Nearest-neighbor tight-binding parameters of HgTe and CdTe. The off-site matrix elements ( $V$ 's) are related to the standard notations for the two-center Slater-Koster<sup>8</sup> approximation as follows:  $V_{s,s} = V_{s,s,\sigma}$ ,  $V_{s,p} = (1/\sqrt{3})V_{s,p,\sigma}$ ,  $V_{p,s} = (-1/\sqrt{3})V_{p,s,\sigma}$ ,  $V_{x,x} = (1/3)(V_{p,p,\sigma} + 2V_{p,p,\pi})$ ,  $V_{x,y} = (1/3)(V_{p,p,\sigma} - V_{p,p,\pi})$ ,  $V_{s^*,p} = (1/\sqrt{3})V_{s^*,p,\sigma}$ ,  $V_{p,s^*} = (-1/\sqrt{3})V_{p,s^*,\sigma}$ .

	CdTe	HgTe
$E_{s,a}$	-8.891	-9.776
$E_{p,a}$	0.915	0.155
$E_{s,c}$	-0.589	-1.404
$E_{p,c}$	4.315	4.300
$4V_{s,s}$	-4.779	-3.267
$4V_{x,x}$	2.355	1.443
$4V_{x,y}$	4.124	3.639
$4V_{s,p}$	1.739	2.412
$4V_{p,s}$	-4.767	-3.243
$E_{s^*,a}$	7.0	6.0
$E_{s^*,c}$	7.5	6.5
$4V_{s^*,p}$	1.949	3.520
$4V_{p,s^*}$	-2.649	-0.323
$\lambda_a$	0.367	0.299
$\lambda_c$	0.013	0.286

<sup>a</sup>J. C. Slater and G. F. Koster, Phys. Rev. **94**, 1498 (1954).

TABLE II. Energies at symmetry points  $\Gamma$ ,  $X$ , and  $L$  (in eV).

Symmetry points	CdTe			HgTe		
	Present	Others		Present	Others	
$\Gamma_{6v}$	-11.07	-11.07 <sup>a</sup>	-10.8 <sup>c</sup>	-10.8	-10.8 <sup>c</sup>	
$\Gamma_{7v}$	-0.89	-0.89 <sup>a</sup> -0.91 <sup>e</sup>	-0.728 <sup>b</sup>	-0.893	-0.893 <sup>b</sup> -0.94 <sup>e</sup>	-1.1 <sup>d</sup>
$\Gamma_{8v}$	0.00	0.00		0.00	0.00	
$\Gamma_{6c}$	1.59	1.59 <sup>a</sup> 1.59 <sup>e</sup>	1.591 <sup>b</sup>	-0.280	-0.280 <sup>b</sup> -0.3 <sup>e</sup>	-0.4 <sup>d</sup>
$\Gamma_{7c}$	5.36	5.36 <sup>a</sup> 6.13 <sup>e</sup>	6.171 <sup>b</sup>	4.179	4.179 <sup>b</sup> 4.9 <sup>e</sup>	5.16 <sup>d</sup>
$\Gamma_{8c}$	5.61	5.61 <sup>a</sup> 6.26 <sup>e</sup>	6.461 <sup>b</sup>	5.040	5.040 <sup>b</sup> 5.41 <sup>e</sup>	6.9 <sup>d</sup>
$X_{6v}$	-9.12	-9.12 <sup>a</sup>		-10.2		
$X_{7v}$	-4.94	-5.05 <sup>a</sup> -3.17 <sup>e</sup>		-3.993	-4.00 <sup>b</sup> -4.0 <sup>e</sup>	-4.5 <sup>d</sup>
$X_{7v}$	-2.08	-1.98 <sup>a</sup> -1.60 <sup>e</sup>	-1.658 <sup>b</sup>	-2.108	-2.056 <sup>b</sup> -1.5 <sup>e</sup>	-1.6 <sup>d</sup>
$X_{6v}$	-1.60	-1.60 <sup>a</sup> -1.14 <sup>e</sup>	-1.320 <sup>b</sup>	-1.826	-1.826 <sup>b</sup> -1.15 <sup>e</sup>	-1.1 <sup>d</sup>
$X_{6c}$	3.48	3.48 <sup>a</sup> 3.85 <sup>e</sup>	3.900 <sup>b</sup>	1.822	1.830 <sup>b</sup> 3.15 <sup>e</sup>	2.8 <sup>d</sup>
$X_{7c}$	3.95	3.95 <sup>a</sup> 4.15 <sup>e</sup>	4.410 <sup>b</sup>	2.705	2.705 <sup>b</sup> 3.9 <sup>e</sup>	5.0 <sup>d</sup>
$X_{6c}$	6.98			6.283		
$X_{7c}$	7.18			6.518		
$L_{6v}$	-9.75	-9.64 <sup>a</sup>		-10.383		
$L_{6v}$	-4.41	-4.73 <sup>a</sup> -3.17 <sup>e</sup>		-3.988		-4.3 <sup>d</sup>
$L_{6v}$	-1.30	-1.18 <sup>a</sup> -0.97 <sup>e</sup>	-1.008 <sup>b</sup>	-1.355	-3.8 <sup>e</sup> -1.298 <sup>b</sup> -1.02 <sup>e</sup>	-1.27 <sup>d</sup>
$L_{45v}$	-0.77	-0.65 <sup>a</sup> -0.4 <sup>e</sup>	-0.546 <sup>b</sup>	-0.755	-0.672 <sup>b</sup> -0.4 <sup>e</sup>	-0.48 <sup>d</sup>
$L_{6c}$	2.47	2.82 <sup>a</sup> 3.0 <sup>e</sup>	3.091 <sup>b</sup>	0.896	1.252 <sup>b</sup> 1.8 <sup>e</sup>	1.5 <sup>d</sup>
$L_{6c}$	5.17	6.18 <sup>a</sup> 6.39 <sup>e</sup>	6.606 <sup>b</sup>	3.869	4.866 <sup>b</sup> 6.0 <sup>e</sup>	6.42 <sup>d</sup>
$L_{45c}$	6.18	6.35 <sup>a</sup> 6.45 <sup>e</sup>	6.695 <sup>b</sup>	5.232	5.194 <sup>b</sup> 6.26 <sup>e</sup>	

<sup>a</sup>Pseudopotential calculations of Ref. 8.

<sup>b</sup>Pseudopotential calculations of Ref. 7.

<sup>c</sup>Photoemission data of Ref. 9.

<sup>d</sup>Orthogonalized plane-wave calculation, H. Overhof, Phys. Status Solidi B 43, 221 (1971).

<sup>e</sup>Pseudopotential calculation, D. J. Chadi, J. P. Walter, M. L. Cohen, Y. Petroff, and M. Balkanski, Phys. Rev. B 5, 3058 (1972).

0.7 and 0.5, respectively. (These values are close to the values 0.8 and 0.6 for III-V's.<sup>4</sup>) These scaling relationships for the host provide rules for the construction of the defect potential  $V$ ; we take  $V$  to be

diagonal in the site representation with diagonal elements equal to

$$V_{i,b} = \beta_i (E_{i,b}^{(\text{defect})} - E_{i,b}^{(\text{host})}), \quad (5)$$



Finally, the spin-orbit coupling breaks the now six-fold degenerate  $T_2$  level into a twofold  $\Gamma_7$  ( $P_{1/2}$ -like) level and a fourfold  $\Gamma_8$  ( $P_{3/2}$ -like) level, since the “good” quantum number is the total angular momentum  $J=L+S$ . The doubly degenerate  $A_1$  level remains doubly degenerate in the presence of the spin-orbit coupling; we denote this level by  $\Gamma_6$  ( $S_{1/2}$ -like) in the double-group notation. These symmetry considerations reduce the secular equation (1a) to three scalar equations for either anion- or cation-substitutional defects:

$$V_p^{-1} = G_0^{(\Gamma_8)}(E) \quad (g=4, P_{3/2}\text{-like}), \quad (6a)$$

$$V_p^{-1} = G_0^{(\Gamma_7)}(E) \quad (g=2, P_{1/2}\text{-like}), \quad (6b)$$

and

$$V_s^{-1} = G_0^{(\Gamma_6)}(E) \quad (g=2, S_{1/2}\text{-like}), \quad (6c)$$

where  $g$  indicates the degeneracy. Details of the derivation are given in Appendix B. The substitutional impurity levels obtained by solving Eqs. (6) for  $\text{Hg}_{(1-x)}\text{Cd}_x\text{Te}$  alloys are shown in Figs. 4–6.

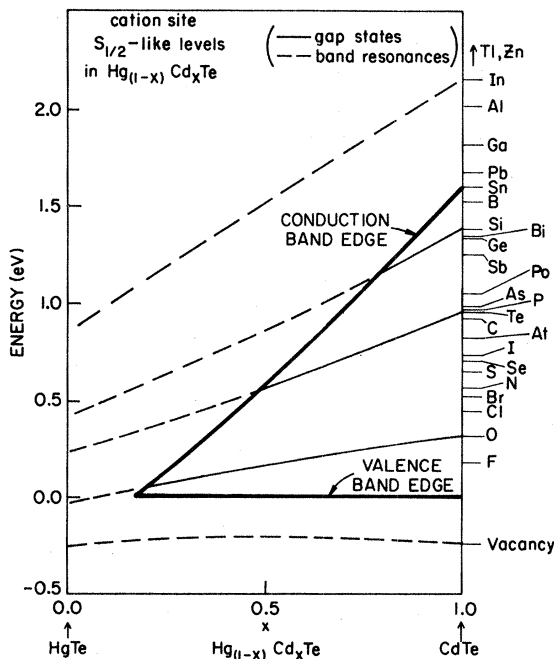


FIG. 4. Predicted  $\Gamma_6$ -symmetric ( $S_{1/2}$ -like) energy levels of cation-site substitutional impurities as a function of the alloy composition  $x$ . The energy levels for all the impurities in CdTe are shown on the right. The trends with alloy composition  $x$  are shown only for selected impurities. The dashed curves indicate resonant levels.

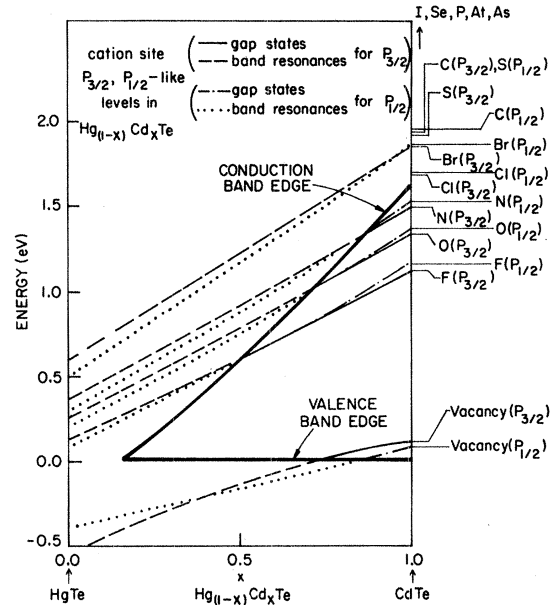


FIG. 5. Predicted  $\Gamma_7$ -symmetric ( $P_{1/2}$ -like) and  $\Gamma_8$ -symmetric ( $P_{3/2}$ -like) energy levels of cation-site substitutional impurities as a function of the alloy composition  $x$ . The energy levels for all the impurities in CdTe are shown on the right. The trends with  $x$  are given only for selected impurities. The  $P_{3/2}$ -like bound and/or resonant states are denoted by solid and/or dashed lines. The  $P_{1/2}$ -like bound and/or resonant states are denoted by chained and/or dotted lines.

### III. RESULTS

One of the most important conclusions is that, in the alloy  $\text{Hg}_{(1-x)}\text{Cd}_x\text{Te}$ , the deep levels have slopes  $dE/dx$  somewhat smaller than  $dE_{\text{gap}}/dx$ . Thus, a defect on a cation site with a level at  $\sim E_{\text{gap}}/2$  in CdTe would tend to remain near the center of the gap for a considerable range of alloy compositions  $x$ . Anion site defects have  $dE/dx$  very small, and so appear to be “attached” to the valence band. The cation-site behavior, by which a gap-center level remains near the gap center for a range of alloy compositions, has been observed by Jones *et al.*<sup>1</sup> for  $0.2 \leq x \leq 0.4$ . Those authors have suggested that their level at  $\sim E_{\text{gap}}/2$ , and possibly their  $\sim 3E_{\text{gap}}/4$  level, may be due to a cation vacancy (presumably singly and doubly charged, respectively), an identification consistent with the present work.

#### A. Cation-site defects

The predictions for cation-site defects are given in Figs. 4 and 5. As an example, consider the im-

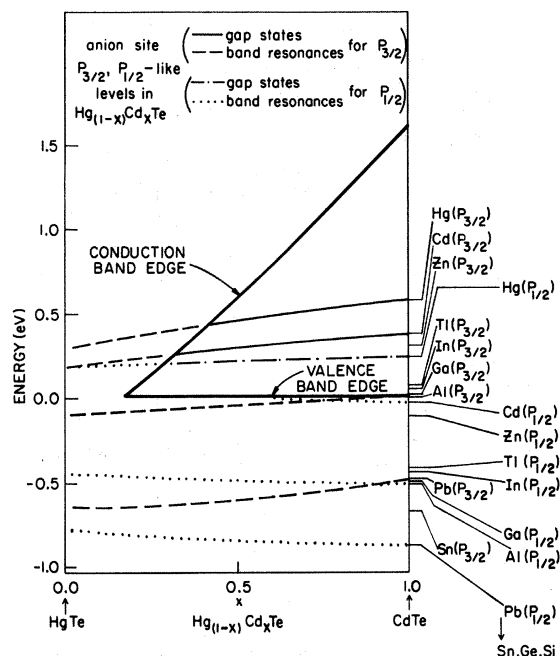


FIG. 6. Predicted  $\Gamma_7$ -symmetric ( $P_{1/2}$ ) and  $\Gamma_8$ -symmetric ( $P_{3/2}$ -like) levels of anion-site substitutional impurities as a function of the alloy composition  $x$ . The energy levels for all the impurities in CdTe are shown on the right. The trends with  $x$  are given only for selected impurities. The anion vacancy "deep" level is a conduction-band resonance above the figure. [The anion vacancy  $\Gamma_6$ -symmetric ( $S_{1/2}$ -like; not shown) level is also a resonance at an energy that would lie above the figure. This resonance would hold two electrons if it were a bound state below the conduction-band edge. Hence the bulk Te-site vacancy produces a shallow double donor.]

purity P in CdTe, which at low concentrations occupies primarily Te ( $P_{\text{Te}}$ ) sites, but at high concentrations is likely to occupy Cd sites as well ( $P_{\text{Cd}}$ ). The  $P_{\text{Cd}}$  impurity has three extra electrons relative to the host and is expected to have a filled  $S_{1/2}$ -like level near 1 eV (Fig. 4) and  $P_{1/2}$ -like and  $P_{3/2}$ -like states resonant with the conduction band (above the top of Fig. 5). (We measure all energies from the valence-band maximum.) These  $P_{1/2}$ - and  $P_{3/2}$ -like resonance states are unable to localize and bind the final (third) electron, since this electron seeks a lower-energy conduction-band state where it can be captured into a shallow level by the long-range Coulomb potential. These shallow states have zero binding energy in the present model, because the long-range Coulomb potential is neglected. If it were included, the electron would occupy an effective-mass-type shallow-donor level.

Thus the defect  $P_{\text{Cd}}$  will show the following electrical properties depending on the background doping: In intrinsic or  $n$ -type material this defect will act as a shallow donor; but in  $p$ -type material the shallow donor electron will be trapped by an acceptor and the 1.0-eV level will become a deep electron trap, if it lies above the Fermi level.

The neutral vacancy  $V_{\text{Cd}}^0$  in CdTe has six electrons (from its Te neighbors); two in the lowest-energy  $S_{1/2}$ -like valence-band resonance (Fig. 4), two in the higher  $P_{1/2}$ -like level, and two in the  $P_{3/2}$ -like level, leaving two empty  $P_{3/2}$ -like levels (Fig. 5). Thus this vacancy is predicted to yield a deep acceptor at 0.12 eV in CdTe (deep in the sense that the localization is primarily produced by the short-range central-cell potential) in good agreement with the very recent theoretical results of Daw *et al.*<sup>11</sup> It should have an inclination to accept one or two electrons, producing the singly or doubly charged vacancy levels. The Coulomb repulsion of these extra electrons, omitted in the present model, would cause the level to move up in energy, and would result in higher energy levels for the singly charged and doubly charged states than for the neutral state. Experimentally the energies of the cation vacancy's different charge states remain uncertain. Levels have been reported at 0.05 eV (Ref. 12) and 0.20 eV (Ref. 13) and the doubly charged vacancy has been reported to lie at 1 eV (Ref. 14); in all cases, however, the assignment of these levels to the  $V_{\text{Cd}}$  has been only tentative.

Further evidence supporting the predictions for cation-site defects in CdTe comes from the pressure-dependent studies on the shallow donor dopants. Iseler *et al.*<sup>15</sup> have found that application of 2 kbar of pressure greatly reduces the conduction electron density for Ga-doped CdTe, indicating that the shallow Ga level is being converted into a deep level. For In-doped samples 10 kbar is necessary, while Al shows no signs of such conversion. The present theory predicts that Ga, In, and Al all have resonance levels near the conduction-band edge in pressure-free CdTe, although we place the In resonance above the Al resonance (see Fig. 4). Each of these column-III impurities has one more electron than Cd. The electron that would naturally occupy this  $S_{1/2}$ -like resonance level decays to the conduction-band minimum, where the long-range Coulomb potential omitted in the present model binds it in an effective-mass shallow donor level. With the application of pressure, the conduction-band edge  $\Gamma$  moves up, expos-

ing the resonance level and a genuine deep electron trap is formed below the shallow donor level. The observation of this dramatic deep-level formation in response to pressure is a triumph of the theory, which places these levels near the borderline of the shallow-deep transition at zero pressure. The present explanation of this phenomenon is natural and requires neither a change in the local geometry of the defect with pressure,<sup>16–18</sup> nor that the deep level be “attached” in an effective-mass approximation sense to a higher conduction-band minimum.<sup>15</sup> The nearest subsidiary conduction-band minimum is at  $L$ , approximately 1 eV higher in energy than the absolute minimum at  $\Gamma$ —too far away for an effective-mass treatment to be credible.

With the experimental evidence for known cation-site defects in CdTe supporting the predictions of the model, we feel some confidence in the predictions for  $\text{Hg}_{(1-x)}\text{Cd}_x\text{Te}$  alloys. For example, the native antisite defect Te in Te-rich alloys should naturally form a doubly occupied  $S_{1/2}$ -like level in the gap (Fig. 4) and a shallow double donor (the  $P_{1/2}$ -like and  $P_{3/2}$ -like resonances are above the figure in Fig. 5). All the impurities from Pb down to F on Fig. 4 and the cation vacancy are candidates for levels at the energies observed by Jones *et al.* in the alloy.

The present work lends support to the assignment of the  $E_{\text{gap}}/2$  level and possibly the  $3E_{\text{gap}}/4$  level in  $\text{Hg}_{(1-x)}\text{Cd}_x\text{Te}$  to the negatively charged cation vacancies. Adding 0.3 to 0.4 eV to the higher of our  $P_{3/2}$ -like or  $P_{1/2}$ -like  $V_{\text{Cd}}^0$  levels, to simulate the effects of electron-electron repulsion in  $V_{\text{Cd}}^-$  (a reasonable charge-state splitting for this material), brings either of these levels of Fig. 5 into general agreement with the  $E_{\text{gap}}/2$  level of Jones *et al.*<sup>1</sup> Similarly, the  $3E_{\text{gap}}/4$  level can be assigned to  $V_{\text{Cd}}^{2-}$ . The remaining isolated substitutional native defect, antisite  $\text{Te}_{\text{Cd}}$  appears not to be a reasonable candidate for these energy levels—it would act as a deep electron trap only if its shallow donor electrons were trapped by compensating levels such as the cation vacancy. In this case the concentration of deep traps would probably be considerably less than the vacancy concentration, while the data show that the defect responsible for this deep level and the cation vacancy occur in concentrations that are roughly equal, within a factor of 10. We must admit however, that an impurity such as  $\text{Te}_{\text{Cd}}$  represents a very extreme case, since four extra electrons must be taken into account, and may in fact lie outside the realm of va-

lidity of the present theory. This is so because in the present theory we have taken the impurity central-cell potential to be proportional to the difference of neutral-atom orbital energies. Thus the theory in its present form is most reliable for impurity atoms that have nearly the same valence structure in the solid (i.e., the same number of electrons in the central-cell volume) as the free atom. The effects of charge transfer and redistribution, which for highly charged defects should be taken into account self-consistently, have not been included. In the absence of a more complete treatment, we cannot rule out the antisite defect as responsible for the levels of Jones *et al.*; indeed in recent private conversations, Jones has expressed the opinion that these may be  $\text{Te}_{\text{Cd}}$  levels.

It appears likely that the  $\text{Te}_{\text{Cd}}$  antisite defect will remain a shallow donor (above the figure in Fig. 5), even if it lies near or at a surface. The  $\text{Te}_{\text{Cd}}$  resonance is so far up in the conduction band that it is unlikely to be driven into the gap by the perturbation of even a surface, based on our experience with surface-defect calculations.<sup>19</sup> Thus, if we accept the Spicer-Bardeen<sup>20</sup> theory of Schottky barrier heights determined by surface Fermi-level pinning and assume that the pinning defect is either an anion vacancy<sup>11</sup> or an antisite defect on the Cd site ( $\text{Te}_{\text{Cd}}$ ),<sup>21</sup> then we would expect the pinning level to lie near the conduction-band edge for all alloy compositions  $x$  in  $\text{Hg}_{(1-x)}\text{Cd}_x\text{Te}$ . This would mean that  $n$ -type  $\text{Hg}_{(1-x)}\text{Cd}_x\text{Te}$  would be expected to form Ohmic contacts with metals, but that  $p$ -type material would have a barrier height equal to the band gap. This result appears not to agree with the observations,<sup>22,23</sup> leading us to conclude that the CdTe Schottky-barrier height is not controlled by either the anion vacancy or  $\text{Te}_{\text{Cd}}$ . The remaining native substitutional surface defects, the Cd vacancy and  $\text{Cd}_{\text{Te}}$ , are potential candidates for the observed Fermi-level pinning deep in the band gap of CdTe, however. Since we find that their bulk levels lie within or near the band gap, they are likely to produce surface levels near or in the gap also. These comments concerning the behavior of defects at or near surfaces must be considered as speculations at this point, however, since a detailed surface calculation will be necessary to predict the precise energy levels.

In bulk CdTe the column-IV impurities Si, Ge, and C are all predicted to produce doubly occupied  $S_{1/2}$ -like deep levels. The column-V defects Bi, Sb, As, and P produce doubly occupied deep  $S_{1/2}$ -like levels and a singly occupied shallow donor level.

The column-VI defects Se, S, and O are predicted to yield very deep occupied  $S_{1/2}$ -like levels and double donors (for Se and S) or a doubly occupied  $P_{3/2}$ -like deep level (for O). All of the bound deep levels in CdTe are "autoionized" and become conduction-band resonances as Hg increasingly replaces Cd in the alloy and the band gap decreases.

The neutral cation vacancy exhibits an especially interesting behavior in the alloy. The deep  $V_{\text{cation}}$  acceptor of CdTe is predicted to merge into the valence band as Cd is increasingly replaced by Hg, producing a "deep" resonance and a shallow double acceptor. The interference of the acceptor states with the conduction-band continuum could explain the anomalous conductivity dips (at  $\approx 2.2$  and 9.5 meV) observed by Finck *et al.*,<sup>24</sup> who speculate that these states are associated with cation-site vacancies. In fact, the present theory is very similar in spirit to that of Liu and Vérier<sup>25</sup> who studied these resonance states theoretically in detail. The fact that neutral cation vacancies in  $\text{Hg}_{(1-x)}\text{Cd}_x\text{Te}$  form shallow acceptors also explains why this material often tends to occur as a  $p$ -type semiconductor.

### B. Anion-site defects

The theoretical results for the anion-site defects are given in Fig. 6. In the present model only the  $P_{3/2}$ -like and  $P_{1/2}$ -like levels of quite electropositive impurities produce levels in the gap; the  $S_{1/2}$ -like levels (not shown) are not found in the gap. Especially noteworthy are the antisite defects Hg and Cd, which are predicted to yield naturally empty  $P_{3/2}$ -like states in the gap and full  $P_{1/2}$ -like levels at or near the valence-band edge.

An interesting feature of the theory is that the derivative  $dE/dx$  for anion-site defects is considerably smaller than for cation-site impurities. The anion-substitutional defects in the alloy tend to parallel the valence-band maximum and have  $dE/dx \approx 0$ . Thus the deep levels observed by Jones *et al.*, which have  $dE/dx$  smaller than  $dE_{\text{gap}}/dx$  by the factors  $\approx \frac{1}{2}$  and  $\approx \frac{3}{4}$ , are more likely to be cation-site defects.

There is a problem with the theory for anion-substitutional defects, however. Isoelectronic O has been reported to act as a luminescent center in CdTe,<sup>26</sup> whereas the theory does not place it in the gap. Furthermore, the pressure experiments of Iseler *et al.*<sup>15</sup> show that Cl and Br must produce resonances only slightly above the conduction-band

edge, because the application of a modest amount of pressure is known to drive these levels into the gap (iodine does not become deep). The theory does predict the observed ordering of these levels<sup>27</sup>: O is deeper than Cl, which is deeper than Br, which is deeper than I; but the predicted level positions are too far away from the gap in absolute energy to explain the observations.

One possible explanation of these experimental facts is that the defect levels assigned to O, Cl, and Br are not associated with isolated substitutional impurities but with some other defects, perhaps pairs consisting of a donor and another defect on a neighboring site. According to the theory, such extended defects might produce levels near the observed energies, and these defects would have the observed ordering.<sup>28</sup> Experiments resolving this issue are needed. While keeping open minds concerning the nature of these defects, we believe that it is prudent, at least for the moment, to assign the discrepancy between theory and data to a deficiency of the theory.

We have examined how alterations of the parameters of the theory might lead to changes of the  $S_{1/2}$ -like level positions for the important isolated substitutional column-VI and -VII defects. These studies lead us to conclude that no reasonable modification of the parameters will bring the theory into quantitative agreement with the O, Cl, and Br data. In order to do that, the  $S_{1/2}$ -like spectral density in the conduction band must be significantly increased so that the levels are repelled downward. However, column-II and column-VI or -VII atoms are very different and their  $s$  atomic energy levels are quite out of resonance. Thus no reasonable change of parameters will lead to the needed transfer of spectral conduction-band strength to the anion-site spectral density. This problem occurs possibly because we have tried to simulate a moderately ionic compound, containing quite polarizable ions, with a basically covalent theory. Effects due to substantial charge rearrangement have been neglected in this theory, and these may be important.

We do not believe that there is much to be gained by developing a more sophisticated theory at this stage. Noting that the present simple theory does successfully predict the relative ordering of the O, Cl, and Br levels, we merely mentally adjust the predictions downward until they coincide with the CdTe impurity data. With this modification, the present theory can function as a useful guide for interpreting data.

## IV. SUMMARY

The chemical trends for the defect levels in  $\text{Hg}_{(1-x)}\text{Cd}_x\text{Te}$  generally appear to be in agreement with the available data. The neutral cation-site defect levels appear to be predicted with an accuracy of typically  $\simeq 0.2$  eV. The anion-site defect levels observed in CdTe have the same general trends that the theory predicts, but we find sizable quantitative discrepancies between the predicted absolute trap energies and data. These discrepancies are systematic, however, and the theory can be adjusted to compensate for them. The theory provides explanations of the principal experimental facts concerning the energies of defect levels in CdTe and the anomalous electrical properties of defects such as the cation vacancy in  $\text{Hg}_{(1-x)}\text{Cd}_x\text{Te}$ . It also seems to provide a very natural explanation of the pressure-dependent shallow-to-deep transition data. We hope that the predictions of Figs. 4–6 will prove helpful for interpreting data.

## ACKNOWLEDGMENTS

We gratefully acknowledge the support of the Office of Naval Research (Contract No. N00014-77-C-0537). We benefited greatly from stimulating

conversations about the data with C. Jones, J. Pollard, and C. Vérié.

## APPENDIX A: TIGHT-BINDING THEORY

In this appendix, we outline the procedure for empirically determining the tight-binding Hamiltonian matrix elements. We begin by constructing for each orbital  $i$  of atom  $b$  ( $b$  is the anion or cation) a Bloch sum of wave vector  $\vec{k}$ :

$$|b, i, \sigma, \vec{k}\rangle = N^{-1/2} \sum_{\vec{R}} \exp[i\vec{k} \cdot (\vec{R} + \vec{\tau}_b)] \times |b, i, \sigma, \vec{R} + \vec{\tau}_b\rangle, \quad (\text{A1})$$

where  $i$  corresponds to one of the  $sp^3s^*$  basis orbitals in the unit cell at  $\vec{R}$  and the spin  $\sigma$  may be either up ( $\uparrow$ ) or down ( $\downarrow$ ). The vector  $\vec{\tau}_b$  is the position vector of the  $b$ th atom in the unit cell [viz.  $(0,0,0)$  for the anion and  $(a_L/4)(1,1,1) = \vec{d}$  for the cation].

Since HgTe and CdTe have large spin-orbit couplings, it is convenient to represent the Hamiltonian in the total angular momentum  $|j, m_j\rangle$  basis rather than the  $|i, \sigma\rangle$  basis ( $i$  labels the orbital angular momentum). The transformation between these two bases is, for example,

$$|b, j=3/2, m_j=3/2, \vec{R}\rangle = -2^{-1/2} (|b, p_x, \uparrow, \vec{R}\rangle + i |b, p_y, \uparrow, \vec{R}\rangle) \quad (\text{A2a})$$

$$|b, j=3/2, m_j=1/2, \vec{R}\rangle = -6^{-1/2} (|b, p_x, \downarrow, \vec{R}\rangle + i |b, p_y, \downarrow, \vec{R}\rangle - 2 |b, p_z, \uparrow, \vec{R}\rangle). \quad (\text{A2b})$$

This transformation results in a diagonalization of the spin-orbit coupling Hamiltonian. We have retained the interactions of the excited  $s^*$  orbital with the valence  $p$  orbital of a neighboring atom, but have neglected for simplicity interactions of the  $s^*$  orbital with the  $s$  and  $s^*$  orbitals of its neighbors. The resultant nearest-neighbor tight-binding Hamiltonian matrix is given in Appendix C.

At high-symmetry points in the Brillouin zone, the matrix becomes block-diagonal. We can thus express the energies at the  $\Gamma$  and  $X$  points in terms of the tight-binding parameters, and empirically determine the parameters, using the known energies at  $\Gamma$  and  $X$  (Table II). The analytic forms at the  $\Gamma$  point [we set  $U_{i,j}^2 = (4V_{i,j})^2$ ] are

$$E(\Gamma_6) = [(E_{s,a} + E_{s,c})/2] \pm [(E_{s,a} - E_{s,c})^2/4 + U_{s,s}^2]^{1/2} \quad (\text{doubly degenerate}), \quad (\text{A3})$$

$$E(\Gamma_7) = [(E_{p,a} + E_{p,c} - 2\lambda_a - 2\lambda_c)/2] \pm [(E_{p,a} - E_{p,c} - 2\lambda_a + 2\lambda_c)^2/4 + U_{x,x}^2]^{1/2} \quad (\text{doubly degenerate}), \quad (\text{A4})$$

and

$$E(\Gamma_8) = [(E_{p,a} + E_{p,c} + \lambda_a + \lambda_c)/2] \pm [(E_{p,a} - E_{p,c} + \lambda_a - \lambda_c)^2/4 + U_{x,x}^2]^{1/2} \quad (\text{fourfold degenerate}). \quad (\text{A5})$$

Using Eqs. (4a), (4b), (A3), (A4), and (A5), we are able to determine the parameters  $E_{s,a}$ ,  $E_{s,c}$ ,  $U_{s,s}$ ,  $E_{p,a}$ ,  $E_{p,c}$ ,  $U_{x,x}$ ,  $\lambda_a$  and  $\lambda_c$  from the energies at the  $\Gamma$  points.

The analysis at the  $X$  point is slightly more complicated due not only to the spin-orbit interaction but also due to the interaction of the excited  $s^*$  orbitals with the valence  $p$  orbitals of its neighbors as well. For the moment, let us neglect the  $s^*-p$  interactions. Then the doubly degenerate  $E(X_6)$  are solutions of the fourth-order equation

TABLE III. Diagonal elements of  $H_{b,b}$ , for either  $b = \text{anion or cation}$ .

$b, s^*, \uparrow$ $E_{s^*,b}$	$b, s^*, \downarrow$ $E_{s^*,b}$	$b, s, \uparrow$ $E_{s,b}$	$b, s, \downarrow$ $E_{s,b}$	$b, 3/2, 3/2$ $E_{p,b} + \lambda_b$
$b, 3/2, 1/2$ $E_{p,b} + \lambda_b$	$b, 3/2, -1/2$ $E_{p,b} + \lambda_b$	$b, 3/2, -3/2$ $E_{p,b} + \lambda_b$	$b, 1/2, 1/2$ $E_{p,b} - 2\lambda_b$	$b, 1/2, -1/2$ $E_{p,b} - 2\lambda_b$

$$\{[E_{p,a} + \lambda_a - E(X_6)][E_{p,c} - \lambda_c - E(X_6)] - U_{x,y}^2\} \{[E_{p,c} - E(X_6)][E_{s,a} - E(X_6)] - U_{s,p}^2\} - 2\lambda_c^2 [E_{p,a} + \lambda_a - E(X_6)][E_{s,a} - E(X_6)] = 0. \quad (\text{A6})$$

This equation is to be regarded as an expression for the unknowns  $U_{x,y}$  and  $U_{s,p}$ . Similarly the energies at  $X_7$  are given by the corresponding equation with the interchange of the anion and cation.

Finally we insert the  $s^*-p$  interactions into the problem. This has the effect of further complicating Eq. (A6) and its  $X_7$  counterpart. Our procedure to minimize these complications is to choose reasonable values for the higher-lying on-site energies  $E_{s,a}^*$  and  $E_{s,c}^*$  and then to solve (say at  $X_6$ ) for  $U_{x,y}$ ,  $U_{s,p}$  and  $U_{s,p}^*$  in an iterative fashion using the values of  $U_{x,y}$  and  $U_{s,p}$  from Eq. (A6) as a starting point. One iteration is usually sufficient to guarantee convergence.

#### APPENDIX B: SOLUTION OF THE SECULAR EQUATION

In this appendix, we outline how the solutions of the secular equation

$$\langle b', j', m_j', \vec{R}' | G_0(E) | b, j, m_j, \vec{R} \rangle = \sum_{n, \vec{k}} \langle b', j', m_j', \vec{R}' | n, \vec{k} \rangle (E - E_{n, \vec{k}})^{-1} \langle n, \vec{k} | b, j, m_j, \vec{R} \rangle. \quad (\text{B3})$$

TABLE IV. The off-diagonal block matrix  $H_{a,c}$ .

	$c, s^*, \uparrow$	$c, s^*, \downarrow$	$c, s, \uparrow$	$c, s, \downarrow$	$c, 3/2, 3/2$
$a, s^*, \uparrow$	0	0	0	0	$-iU_{s^*,p}g_4/\sqrt{2}$
$a, s^*, \downarrow$	0	0	0	0	0
$a, s, \uparrow$	0	0	$U_{s,s}g_0$	0	$-iU_{s,p}g_4/\sqrt{2}$
$a, s, \downarrow$	0	0	0	$U_{s,s}g_0$	0
$a, 3/2, 3/2$	$-iU_{p,s^*}g_5/\sqrt{2}$	0	$-iU_{p,s}g_5/\sqrt{2}$	0	$U_{x,x}g_0$
$a, 3/2, 1/2$	$-\sqrt{2}U_{p,s^*}g_3/\sqrt{3}$	$-iU_{p,s^*}g_5/\sqrt{6}$	$-\sqrt{2}U_{p,s}g_3/\sqrt{3}$	$-iU_{p,s}g_5/\sqrt{6}$	$-U_{x,y}g_5/\sqrt{3}$
$a, 3/2, -1/2$	$-iU_{p,s^*}g_4/\sqrt{6}$	$-\sqrt{2}U_{p,s^*}g_3/\sqrt{3}$	$-iU_{p,s}g_4/\sqrt{6}$	$-\sqrt{2}U_{p,s}g_3/\sqrt{3}$	$-iU_{x,y}g_3/\sqrt{3}$
$a, 3/2, -3/2$	0	$-iU_{p,s^*}g_4/\sqrt{2}$	0	$-iU_{p,s}g_4/\sqrt{2}$	0
$a, 1/2, 1/2$	$U_{p,s^*}g_3/\sqrt{3}$	$-iU_{p,s^*}g_5/\sqrt{3}$	$U_{p,s}g_3/\sqrt{3}$	$-iU_{p,s}g_5/\sqrt{3}$	$U_{x,y}g_5/\sqrt{6}$
$a, 1/2, -1/2$	$iU_{p,s^*}g_4/\sqrt{3}$	$-U_{p,s^*}g_3/\sqrt{3}$	$iU_{p,s}g_4/\sqrt{3}$	$-U_{p,s}g_3/\sqrt{3}$	$i\sqrt{2}U_{x,y}g_3/\sqrt{3}$

are obtained.

The Green's function  $G_0(E) = (E - H_0)^{-1}$  can be expressed in terms of the eigenvalues and the eigenfunctions of  $H_0$ , by inserting a complete set of states

$$G_0(E) = \sum_{n, \vec{k}} |n, \vec{k}\rangle (E - E_{n, \vec{k}})^{-1} \langle n, \vec{k}|, \quad (\text{B2})$$

where  $|n, \vec{k}\rangle$  is a linear combination of the Bloch sums  $|b, j, m_j, \vec{k}\rangle$  [Eq. (A1)], but in the total angular-momentum basis set [Eq. (A2)].

The general matrix element of  $G_0(E)$  in the site basis  $|b, j, m_j, \vec{R}\rangle$  is then

Since the off-site matrix elements of the substitutional impurity potential  $V = H - H_0$  vanish, the secular equation (B1) need only be solved for  $\vec{R} = \vec{R}' = 0$ . Thus the secular equation reduces to

$$\langle b, j', m_j', \vec{0} | 1 - G_0(E)V | b, j, m_j, \vec{0} \rangle = 0, \quad (\text{B4})$$

or

$$\delta_{jj'} \delta_{m_j m_j'} V_j^{-1} - \langle b, j', m_j', \vec{0} | G_0(E) | b, j, m_j, \vec{0} \rangle = 0, \quad (\text{B5})$$

for the anion site ( $b = a$ ) impurity or the cation site ( $b = c$ ) impurity. Finally, since  $G_0$  has the same symmetry as  $H_0$ , we have

$$\langle b, j', m_j', \vec{0} | G_0(E) | b, j, m_j, \vec{0} \rangle \propto \delta_{jj'} \delta_{m_j m_j'}, \quad (\text{B6})$$

diagonal in  $j$  and  $m_j$ , and independent of  $m_j$ . Thus we have

$$V_j^{-1} - \langle b, j, m_j, \vec{0} | G_0(E) | b, j, m_j, \vec{0} \rangle = 0. \quad (\text{B7})$$

For both of  $b = a$  and  $b = c$  the equations are

$$V_{P_{3/2}}^{-1} = G_0^{(P_{3/2})}(E) \equiv G_0^{(\Gamma_8)}(E), \quad (\text{B8a})$$

$$V_{P_{1/2}}^{-1} = G_0^{(P_{1/2})}(E) \equiv G_0^{(\Gamma_7)}(E), \quad (\text{B8b})$$

$$V_{S_{1/2}}^{-1} = G_0^{(S_{1/2})}(E) \equiv G_0^{(\Gamma_6)}(E), \quad (\text{B8c})$$

where we have

$$\langle b, j, m_j, \vec{0} | G_0(E) | b, j, m_j, \vec{0} \rangle \equiv G_0^{(j)}(E).$$

In the text, we ignore the spin-orbit coupling for the defect potential; hence we have

$$V_{P_{3/2}} = V_{P_{1/2}} \equiv V_p \text{ and } V_{S_{1/2}} \equiv V_s.$$

#### APPENDIX C: THE TWENTY-STATE HAMILTONIAN

The  $\vec{k}$ -space Hamiltonian in the 20-state basis can be written in block form, with block  $H_{a,a}$ ,  $H_{a,c}$ , and  $H_{c,c}$ :

$$H_0(\vec{k}) = \begin{bmatrix} H_{a,a} & H_{a,c} \\ H_{a,c}^\dagger & H_{c,c} \end{bmatrix}.$$

The block matrices  $H_{a,a}$  and  $H_{c,c}$  are diagonal, with the elements given in Table III.

The off-diagonal block matrix  $H_{a,c}$  is given in Table IV. Here we have

$$g_0(\vec{k}) = \cos(k_x a_L / 4) \cos(k_y a_L / 4) \cos(k_z a_L / 4) - i \sin(k_x a_L / 4) \sin(k_y a_L / 4) \sin(k_z a_L / 4),$$

$$g_1(\vec{k}) = -\cos(k_x a_L / 4) \sin(k_y a_L / 4) \sin(k_z a_L / 4) + i \sin(k_x a_L / 4) \cos(k_y a_L / 4) \cos(k_z a_L / 4),$$

TABLE IV. (Continued.)

$c, 3/2, 1/2$	$c, 3/2, -1/2$	$c, 3/2, -3/2$	$c, 1/2, 1/2$	$c, 1/2, -1/2$
$\sqrt{2}U_{s^*,p}g_3/\sqrt{3}$	$-iU_{s^*,p}g_5/\sqrt{6}$	0	$-U_{s^*,p}g_3/\sqrt{3}$	$iU_{s^*,p}g_5/\sqrt{3}$
$-iU_{s^*,p}g_4/\sqrt{6}$	$\sqrt{2}U_{s^*,p}g_3/\sqrt{3}$	$-iU_{s^*,p}g_5/\sqrt{2}$	$-iU_{s^*,p}g_4/\sqrt{3}$	$U_{s^*,p}g_3/\sqrt{3}$
$\sqrt{2}U_{s,p}g_3/\sqrt{3}$	$-iU_{s,p}g_5/\sqrt{6}$	0	$-U_{s,p}g_3/\sqrt{3}$	$iU_{s,p}g_5/\sqrt{3}$
$-iU_{s,p}g_4/\sqrt{6}$	$\sqrt{2}U_{s,p}g_3/\sqrt{3}$	$-iU_{s,p}g_5/\sqrt{2}$	$-iU_{s,p}g_4/\sqrt{3}$	$U_{s,p}g_3/\sqrt{3}$
$-U_{x,y}g_4/\sqrt{3}$	$iU_{x,y}g_3/\sqrt{3}$	0	$U_{x,y}g_4/\sqrt{6}$	$-i\sqrt{2}U_{x,y}g_3/\sqrt{3}$
$U_{x,x}g_0$	0	$iU_{x,y}g_3/\sqrt{3}$	0	$-U_{x,y}g_4/\sqrt{2}$
0	$U_{x,x}g_0$	$U_{x,y}g_4/\sqrt{3}$	$-U_{x,y}g_5/\sqrt{2}$	0
$-iU_{x,y}g_3/\sqrt{3}$	$U_{x,y}g_5/\sqrt{3}$	$U_{x,x}g_0$	$-i\sqrt{2}U_{x,y}g_3/\sqrt{3}$	$U_{x,y}g_5/\sqrt{6}$
0	$-U_{x,y}g_4/\sqrt{2}$	$i\sqrt{2}U_{x,y}g_3/\sqrt{3}$	$U_{x,x}g_0$	0
$-U_{x,y}g_5/\sqrt{2}$	0	$U_{x,y}g_4/\sqrt{6}$	0	$U_{x,x}g_0$

$$g_2(\vec{k}) = -\sin(k_x a_L/4)\cos(k_y a_L/4)\sin(k_z a_L/4) + i\cos(k_x a_L/4)\sin(k_y a_L/4)\cos(k_z a_L/4),$$

$$g_3(\vec{k}) = -\sin(k_x a_L/4)\sin(k_y a_L/4)\cos(k_z a_L/4) + i\cos(k_x a_L/4)\cos(k_y a_L/4)\sin(k_z a_L/4),$$

$$g_4(\vec{k}) = g_2(\vec{k}) - ig_1(\vec{k}), \quad \text{and} \quad g_5(\vec{k}) = g_2(\vec{k}) + ig_1(\vec{k}).$$

The parameters  $U$  are related to the nearest-neighbor matrix elements  $V$  as follows:

$$U_{s,s} = 4V_{s,s} = 4\langle a, s, \sigma, \vec{0} | H_0 | c, s, \sigma, \vec{d} \rangle,$$

$$U_{x,y} = 4V_{x,y} = 4\langle a, p_x, \sigma, \vec{0} | H_0 | c, p_y, \sigma, \vec{d} \rangle,$$

$$U_{x,x} = 4V_{x,x} = 4\langle a, p_x, \sigma, \vec{0} | H_0 | c, p_x, \sigma, \vec{d} \rangle,$$

$$U_{s,p} = 4V_{s,p} = 4\langle a, s, \sigma, \vec{0} | H_0 | c, p_j, \sigma, \vec{d} \rangle,$$

$$U_{p,s} = -4V_{p,s} = -4\langle a, p_j, \sigma, \vec{0} | H_0 | c, s, \sigma, \vec{d} \rangle,$$

$$U_{s^*,p} = 4V_{s^*,p} = 4\langle a, s^*, \sigma, \vec{0} | H_0 | c, p_j, \sigma, \vec{d} \rangle,$$

and

$$U_{p,s^*} = -4V_{p,s^*} = -4\langle a, p_j, \sigma, \vec{0} | H_0 | c, s^*, \sigma, \vec{d} \rangle,$$

where  $j = x, y, \text{ or } z$ . We also have  $U_{x,y} = U_{y,z} = U_{z,x}$  and  $U_{x,x} = U_{y,y} = U_{z,z}$ . Note the phase convention that we have adopted in defining the  $U$ 's.

- <sup>1</sup>C. E. Jones, V. Nair, and D. L. Polla, *Appl. Phys. Lett.* **39**, 248 (1981).
- <sup>2</sup>H. P. Hjalmarson, P. Vogl, D. J. Wolford, and J. D. Dow, *Phys. Rev. Lett.* **44**, 810 (1980).
- <sup>3</sup>W. Y. Hsu, J. D. Dow, D. J. Wolford, and B. G. Streetman, *Phys. Rev. B* **16**, 1597 (1977).
- <sup>4</sup>P. Vogl, H. P. Hjalmarson, and J. D. Dow, *J. Phys. Chem. Solids* (in press).
- <sup>5</sup>W. A. Harrison, *Phys. Rev. B* **8**, 4487 (1973).
- <sup>6</sup>D. J. Chadi, *Phys. Rev. B* **16**, 790 (1977).
- <sup>7</sup>S. Katsuki and M. Kunimune, *J. Phys. Soc. Jpn.* **31**, 415 (1971).
- <sup>8</sup>J. R. Chelikowsky and M. L. Cohen, *Phys. Rev. B* **14**, 556 (1976).
- <sup>9</sup>N. J. Shevchik, J. Tejada, M. Cardona, and D. W. Langer, *Phys. Status Solidi B* **52**, 87 (1973).
- <sup>10</sup>See, for example, C. W. Myles and J. D. Dow, *Phys. Rev. B* **19**, 4939 (1979), and references therein.
- <sup>11</sup>M. S. Daw, D. L. Smith, C. A. Swarts, and T. C. McGill, *J. Vac. Sci. Technol.* **19**, 508 (1981).
- <sup>12</sup>M. R. Lorenz and B. Segall, *Phys. Lett.* **7**, 18 (1963).
- <sup>13</sup>S. Yamada, *J. Phys. Soc. Jpn.* **15**, 1940 (1960).
- <sup>14</sup>D. de Nobel, *Philips Res. Rep.* **14**, 361 (1959); F. A. Kröger, *The Chemistry of Imperfect Crystals*, 2nd ed. (North-Holland, Amsterdam, 1974).
- <sup>15</sup>G. W. Iseler, J. A. Kafalas, A. J. Strauss, H. F. MacMillan, and R. H. Bube, *Solid State Commun.* **10**, 619 (1972).
- <sup>16</sup>D. L. Losee, R. P. Khosla, D. K. Ranadive, and F. J. T. Smith, *Solid State Commun.* **13**, 819 (1973).
- <sup>17</sup>M. Baj, L. Dmowski, M. Kończykowski, and S. Porowski, *Phys. Status Solidi A* **33**, 421 (1976).
- <sup>18</sup>Lattice relaxation, which we have neglected, very likely plays some role in affecting the conductivity experiments of Refs. 15–17, because a time delay is observed between the application or removal of pressure

and the alteration of the conductivity. This delay suggests that the conductivity anomaly is not entirely electronic in origin.

- <sup>19</sup>R. E. Allen and J. D. Dow, *J. Vac. Sci. Technol.* **19**, 383 (1981).
- <sup>20</sup>W. E. Spicer, I. Lindau, P. Skeath, C. Y. Su, and P. Chye, *Phys. Rev. Lett.* **44**, 420 (1980); J. Bardeen, *Phys. Rev.* **71**, 717 (1947).
- <sup>21</sup>R. E. Allen and J. D. Dow, *Phys. Rev. B* **25**, 1205 (1982).
- <sup>22</sup>C. A. Mead and W. G. Spitzer, *Phys. Rev.* **134**, A713 (1964); C. Menezes, F. Sanchez-Sinencio, J. S. Helman, R. Williams, and J. Dresner, *Appl. Phys. Lett.* **31**, 16 (1977); T. P. Humphreys, M. H. Patterson, and R. H. Williams, *J. Vac. Sci. Technol.* **17**, 886 (1980).
- <sup>23</sup>Our calculations show that the anion vacancy also produces a shallow bulk donor, which is likely to remain shallow at the surface; hence, this defect could also produce Fermi-level pinning near the conduction band edge in  $\text{Hg}_{(1-x)}\text{Cd}_x\text{Te}$ . Recently, M. S. Daw, D. L. Smith, C. A. Swarts, and T. C. McGill (Ref. 11) have reported on this vacancy in CdTe; their results for this material and ours agree.
- <sup>24</sup>C. Finck, S. Otmegzguine, G. Weill, and C. Vérié, in *Proceedings of the Eleventh International Conference on the Physics of Semiconductors, Warsaw, 1972*, edited by M. Miqsck (Polish Scientific Warsaw, 1972), p. 944.
- <sup>25</sup>L. Liu and C. Vérié, *Phys. Rev. Lett.* **37**, 453 (1976).
- <sup>26</sup>N. V. Agrinskaya, G. I. Aleksandrova, E. N. Arkad'eva, B. A. Atabekov, O. A. Matveev, G. B. Perepelova, S. V. Prokof'ev, and G. I. Shmanenkova, *Fiz. Tekh. Poluprovodn.* **8**, 317 (1974) [*Sov. Phys.—Semicond.* **8**, 202 (1974)].
- <sup>27</sup>The predicted ordering of the Te site  $S_{1/2}$ -like levels, beginning  $\simeq 1$  eV above the conduction-band edge and

going to higher energy is vacancy, F, O, Cl, Br, N, S, Se, I, At, and C. The other  $sp^3$ -bonded impurities are electropositive with respect to Te, and would produce valence-band resonances far below the valence-band maximum: Hg, Cd, Zn, Tl, In, Al, Ga, Pb, . . .

<sup>28</sup>O. F. Sankey, H. P. Hjalmarson, J. D. Dow, D. J. Wolford and B. G. Streetman, *Phys. Rev. Lett.* **45**, 1656 (1980); O. F. Sankey and J. D. Dow, *Appl. Phys. Lett.* **38**, 685 (1981).